



# Infiltration of COX-2–expressing macrophages is a prerequisite for IL-1 $\beta$ –induced neovascularization and tumor growth

Shintaro Nakao,<sup>1,2</sup> Takashi Kuwano,<sup>1</sup> Chikako Tsutsumi-Miyahara,<sup>2</sup> Shu-ichi Ueda,<sup>1</sup> Yusuke N. Kimura,<sup>3,4</sup> Shinjiro Hamano,<sup>5</sup> Koh-hei Sonoda,<sup>2</sup> Yasuo Saijo,<sup>6</sup> Toshihiro Nukiwa,<sup>6</sup> Robert M. Strieter,<sup>7</sup> Tatsuro Ishibashi,<sup>2</sup> Michihiko Kuwano,<sup>3,4</sup> and Mayumi Ono<sup>1,3</sup>

<sup>1</sup>Department of Medical Biochemistry, <sup>2</sup>Department of Ophthalmology, Graduate School of Medical Sciences, and <sup>3</sup>Collabo-Station II, Kyushu University, Fukuoka, Japan. <sup>4</sup>Research Center of Innovative Cancer Therapy, Kurume University, Kurume, Japan. <sup>5</sup>Department of Parasitology, Graduate School of Medical Sciences, Kyushu University, Fukuoka, Japan. <sup>6</sup>Department of Respiratory Oncology and Molecular Medicine, Institute of Development, Aging, and Cancer, Tohoku University, Sendai, Japan. <sup>7</sup>Department of Medicine, Division of Pulmonary and Critical Care Medicine, David Geffen School of Medicine, University of California at Los Angeles, Los Angeles, California, USA.

**Inflammatory angiogenesis is a critical process in tumor progression and other diseases. The inflammatory cytokine IL-1 $\beta$  promotes angiogenesis, tumor growth, and metastasis, but its mechanisms remain unclear. We examined the association between IL-1 $\beta$ –induced angiogenesis and cell inflammation. IL-1 $\beta$  induced neovascularization in the mouse cornea at rates comparable to those of VEGF. Neutrophil infiltration occurred on day 2. Macrophage infiltration occurred on days 4 and 6. The anti-Gr-1 Ab-induced depletion of infiltrating neutrophils did not affect IL-1 $\beta$ – or VEGF-induced angiogenesis. The former was reduced in monocyte chemoattractant protein-1–deficient (MCP-1<sup>-/-</sup>) mice compared with wild-type mice. After day 4, clodronate liposomes, which kill macrophages, reduced IL-1 $\beta$ –induced angiogenesis and partially inhibited VEGF-induced angiogenesis. Infiltrating macrophages near the IL-1 $\beta$ –induced neovasculature were COX-2 positive. Lewis lung carcinoma cells expressing IL-1 $\beta$  (LLC/IL-1 $\beta$ ) developed neovasculature with macrophage infiltration and enhanced tumor growth in wild-type but not MCP-1<sup>-/-</sup> mice. A COX-2 inhibitor reduced tumor growth, angiogenesis, and macrophage infiltration in LLC/IL-1 $\beta$ . Thus, macrophage involvement might be a prerequisite for IL-1 $\beta$ –induced neovascularization and tumor progression.**

## Introduction

Angiogenesis, which involves a balance of promoters and inhibitors, is enhanced in many diseases (1). However, clinical trials with antiangiogenic factors have been less effective than predicted from mouse models, suggesting angiogenesis may be orchestrated by a more complex set of growth factors, cytokines, and cell types (2).

IL-1 $\beta$  is an inflammatory cytokine that might modulate angiogenesis by directly interacting with vascular endothelial cells or enhancing the production of proangiogenic factors via paracrine control (3–5). IL-1 $\beta$  stimulates endothelial cell migration and proliferation, adhesion-molecule expression, inflammatory mediator production, and leukocyte recruitment. It is required for tumor growth, metastasis, and angiogenesis in several animal models (6–8). IL-1 $\beta$  receptor antagonists inhibit angiogenesis and tumor development, suggesting that IL-1 $\beta$  receptor signaling is involved in inflammation and tumor growth (9). Song et al. reported that IL-1 $\alpha$  reduced tumorigenicity by inducing

antitumor immunity, while IL-1 $\beta$  promoted invasiveness, tumor angiogenesis, and host immune suppression (10).

During inflammation, vessel formation allows the rapid influx of nutrients and inflammatory cells, supplying key cytokines and growth factors to the angiogenic bed. Neutrophils, which modulate the host immune response, appear during angiogenesis induced by corneal injury or bFGF (11) and produce several proangiogenic cytokines. Monocytes, which differentiate into macrophages, migrate to inflammatory sites in response to chemotactic factors (12). Monocyte chemoattractant protein-1–deficient (MCP-1<sup>-/-</sup>) mice that cannot recruit monocytes are resistant to experimental autoimmune encephalomyelitis and display delayed wound re-epithelization (13–15). Activated macrophages function in pathological hemangiogenesis and lymphangiogenesis in choroidal neovascularization, in advanced atherosclerosis and inflammation, and in malignant tumor development (16–19). Macrophages in the tumor stroma are closely correlated with neovascularization and poor prognosis in human cancers, including breast (20, 21), glioma (22), prostate (23), cervix (24, 25), lung (26), bladder (27), and melanoma (5, 28). Activated macrophage infiltration might influence the angiogenesis cascade by producing growth stimulators and inhibitors, cytokines, and proteolytic enzymes (20, 29, 30). However, it remains unclear how infiltrating macrophages function in angiogenesis and tumor enlargement along with the inflammatory response.

We previously demonstrated that IL-1 $\beta$  induced angiogenesis in vitro and in vivo through the COX-2–prostanoid pathway (31).

**Nonstandard abbreviations used:** Cl<sub>2</sub>MDP-LIP, clodronate liposome; CXCL1, CXC chemokine ligand 1; CXCR2, CXC chemokine receptor 2; DFU, 5,5-dimethyl-3-(3-fluorophenyl)-4-(4-methylsulphonyl)phenyl-2((5H)-furanone; ENA-78, epithelial neutrophil-activating peptide-78; LLC, Lewis lung carcinoma; LLC/IL-1 $\beta$ , LLC cells expressing IL-1 $\beta$ ; LLC/neo, LLC cells expressing *neo*<sup>R</sup>; MCP-1, monocyte chemoattractant protein-1; MIP-2, macrophage inflammatory protein 2; PBS-LIP, PBS-containing liposome; s.c., subconjunctival(ly); TXA<sub>2</sub>, thromboxane A<sub>2</sub>.

**Conflict of interest:** The authors have declared that no conflict of interest exists.

**Citation for this article:** *J. Clin. Invest.* 115:2979–2991 (2005). doi:10.1172/JCI23298.

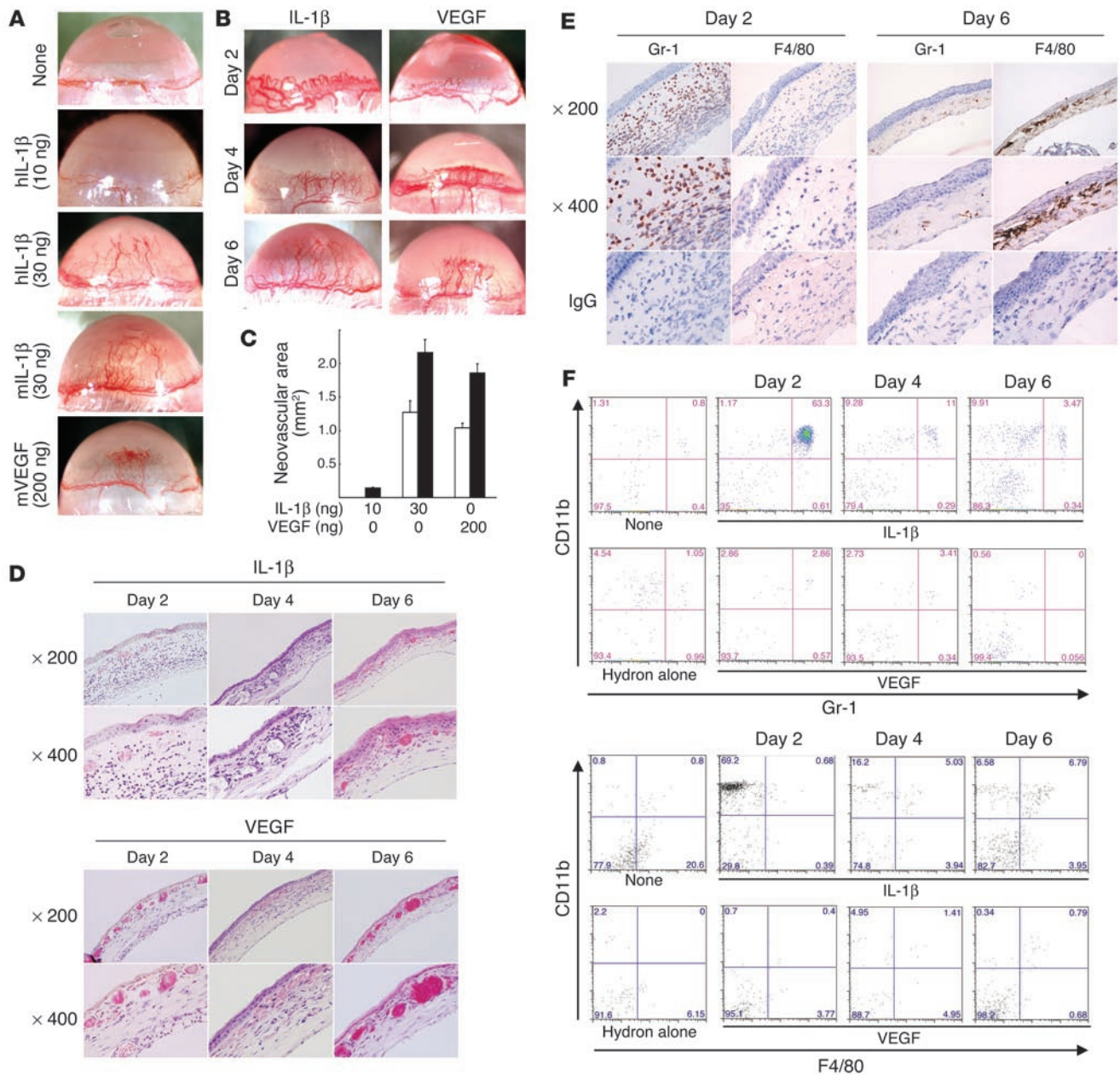


**Figure 1**

IL-1 $\beta$ - and VEGF-induced angiogenesis and inflammatory cell infiltration in mouse corneas. (A) Neovascularization 6 days after implanting Hydrion pellets containing human or mouse IL-1 $\beta$  or mouse VEGF at the doses shown into male BALB/c mouse corneas. hIL-1 $\beta$ , human IL-1 $\beta$ ; mL-1 $\beta$ , mouse IL-1 $\beta$ ; mVEGF, mouse VEGF. (B) Corneal neovascularization induced by human IL-1 $\beta$  (30 ng) or mouse VEGF (200 ng) at the indicated time points. (C) Quantitative analysis of neovascularization on days 4 (white bars) and 6 (black bars). Areas are expressed in mm<sup>2</sup>. Bars show the mean  $\pm$  SD of independent experiments ( $n = 6$  or  $7$ ). (D) Corneas implanted with IL-1 $\beta$  or VEGF stained by H&E at the indicated time points. (E) Corneal sections on days 2 or 6 after IL-1 $\beta$ -pellet implantation, labeled immunohistochemically (brown) for Gr-1, which was detected in infiltrating cells on days 2 and 6, and F4/80, which was detected on day 6. (F) FACS analysis of infiltrating cells from IL-1 $\beta$ - or VEGF-implanted corneas ( $n = 5$ ) at the indicated times. Cells were stained with PE-CD11b mAb and FITC-Gr-1 or FITC-F4/80 mAb. The percentages of infiltrating CD11b<sup>+</sup>Gr-1<sup>+</sup> cells in IL-1 $\beta$ -implanted corneas were 53.5%  $\pm$  10.4% (day 2), 15.8%  $\pm$  4.9% (day 4), and 3.15%  $\pm$  0.27% (day 6). The percentages of infiltrating CD11b<sup>+</sup>Gr-1<sup>+</sup> cells in VEGF-implanted corneas were 2.99%  $\pm$  1.37% (day 2), 1.95%  $\pm$  0.75% (day 4), and 1.08%  $\pm$  0.74% (day 6). The percentages of infiltrating CD11b<sup>+</sup>F4/80<sup>+</sup> cells in IL-1 $\beta$ -implanted corneas were 1.85%  $\pm$  1.28% (day 2), 5.56%  $\pm$  1.61% (day 4), and 5.52%  $\pm$  1.14% (day 6). The percentages of infiltrating CD11b<sup>+</sup>F4/80<sup>+</sup> cells in VEGF-implanted corneas were 0.81%  $\pm$  0.47% (day 2), 1.30%  $\pm$  1.03% (day 4), and 1.90%  $\pm$  0.98% (day 6).

Several reports showed that IL-1 $\beta$  enhanced tumor growth and metastasis via angiogenesis along with inflammatory cell infiltration around cancer cells (6, 8). We observed the infiltration of

COX-2-positive cells around IL-1 $\beta$ -induced neovasculature (31). The current study investigated how IL-1 $\beta$ -induced angiogenesis was coordinated with the infiltration of inflammatory cells.





## Results

**IL-1 $\beta$ -induced angiogenesis in mouse corneas.** We implanted hydron pellets impregnated with human IL-1 $\beta$ , mouse IL-1 $\beta$ , or mouse VEGF into mouse corneas, and outgrowth of new blood vessels was observed 6 days later. While 10 ng human IL-1 $\beta$  induced negligible angiogenesis, 30 ng human and 30 ng mouse IL-1 $\beta$  induced levels of angiogenesis similar to those induced by 200 ng VEGF.

We next examined corneal neovascularization induced by IL-1 $\beta$  or VEGF in more detail (Figure 1B). On day 2, vascular loop structures appeared in IL-1 $\beta$ - and VEGF-implanted corneas; the former showed greater dilation than the latter. On day 4, these structures disappeared from the IL-1 $\beta$ -treated corneas, and both IL-1 $\beta$  and VEGF induced corneal neovascularization extending halfway between the limbus and the pellets. On day 6, the corneal neovas-

cularization reached the pellets. Quantitative analysis demonstrated that 30 ng IL-1 $\beta$  and 200 ng VEGF induced comparable levels of corneal neovascularization on days 4 and 6 (Figure 1C).

**Infiltration of inflammatory cells into mouse corneas in response to IL-1 $\beta$ .** We examined inflammatory cell infiltration into the cornea in response to IL-1 $\beta$  using histological examination (Figure 1, D and E) and flow cytometry (Figure 1F). On day 2, histological sections revealed prominent inflammatory cell infiltration and edema of the stromal layer around the neovascularization. These effects were absent after VEGF implantation. On day 6, numerous inflammatory cells were present in the IL-1 $\beta$ -implanted cornea whereas few were seen in the VEGF-implanted cornea (Figure 1D).

The cell types infiltrating the IL-1 $\beta$ -induced neovascularure in the cornea were identified using specific mAbs against neutrophils

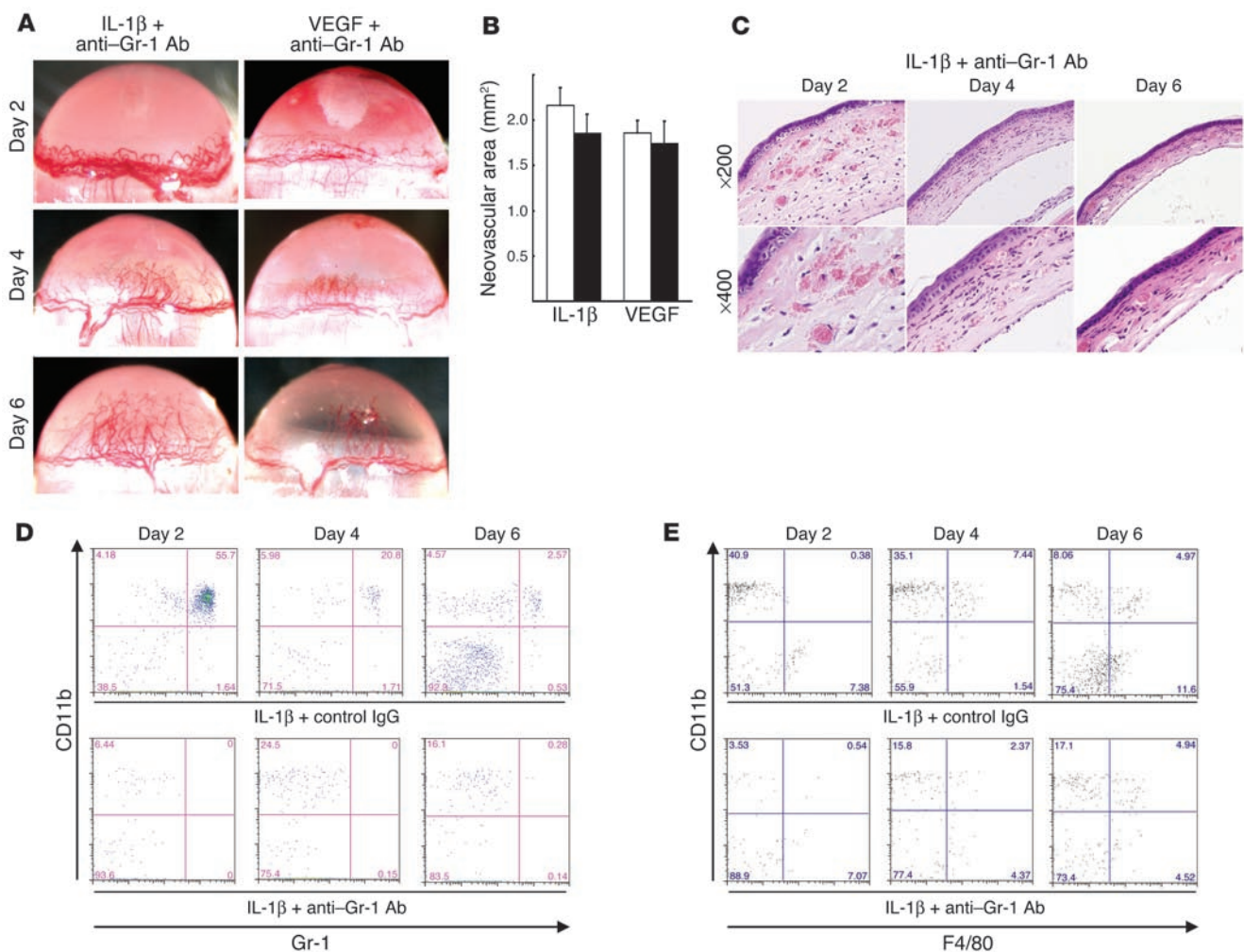


### Figure 2

The role of neutrophils in IL-1 $\beta$ - or VEGF-induced angiogenesis. **(A)** BALB/c mice received 200  $\mu$ g neutralizing anti-Gr-1 mAb i.p. on days -1, 1, 3, and 5. Hydron pellets containing IL-1 $\beta$  (30 ng) or VEGF (200 ng) were implanted into the corneas on day 0. Corneal vessels in the region of the pellet implants were photographed at the indicated time points. **(B)** Anti-Gr-1 mAb did not suppress IL-1 $\beta$ - or VEGF-induced corneal neovascularization. Corneal neovascularization 6 days after treatment with anti-Gr-1 mAb (black bars) or control IgG (white bars) was quantified by area, in mm<sup>2</sup>. The bars show means  $\pm$  SD of independent experiments ( $n = 3$  or 4). **(C)** Corneas implanted with IL-1 $\beta$  stained by H&E at the indicated time points. Anti-Gr-1 mAb did not affect IL-1 $\beta$ -induced corneal edema on day 2. **(D)** FACS analysis of infiltrating cells after IL-1 $\beta$  implantation ( $n = 5$ ) and treatment with anti-Gr-1 mAb or control IgG at the indicated times. The cells were stained with PE-CD11b mAb or FITC-Gr-1. The percentages of CD11b<sup>+</sup>Gr-1<sup>+</sup> cells in IL-1 $\beta$ -implanted corneas of anti-Gr-1 mAb-treated mice were 0.25%  $\pm$  0.22% (day 2), 0.11%  $\pm$  0.1% (day 4), and 0.28%  $\pm$  0.37% (day 6). **(E)** FACS analysis of infiltrating cells from 5 IL-1 $\beta$ -implanted corneas treated with anti-Gr-1 mAb or control IgG at the indicated times. Cells were stained with PE-CD11b mAb or FITC-F4/80. The percentages of CD11b<sup>+</sup>F4/80<sup>+</sup> cells in IL-1 $\beta$ -implanted corneas of anti-Gr-1 mAb-treated mice were 1.71%  $\pm$  1.04% (day 2), 4.36%  $\pm$  1.20% (day 4), and 5.57%  $\pm$  1.34% (day 6).

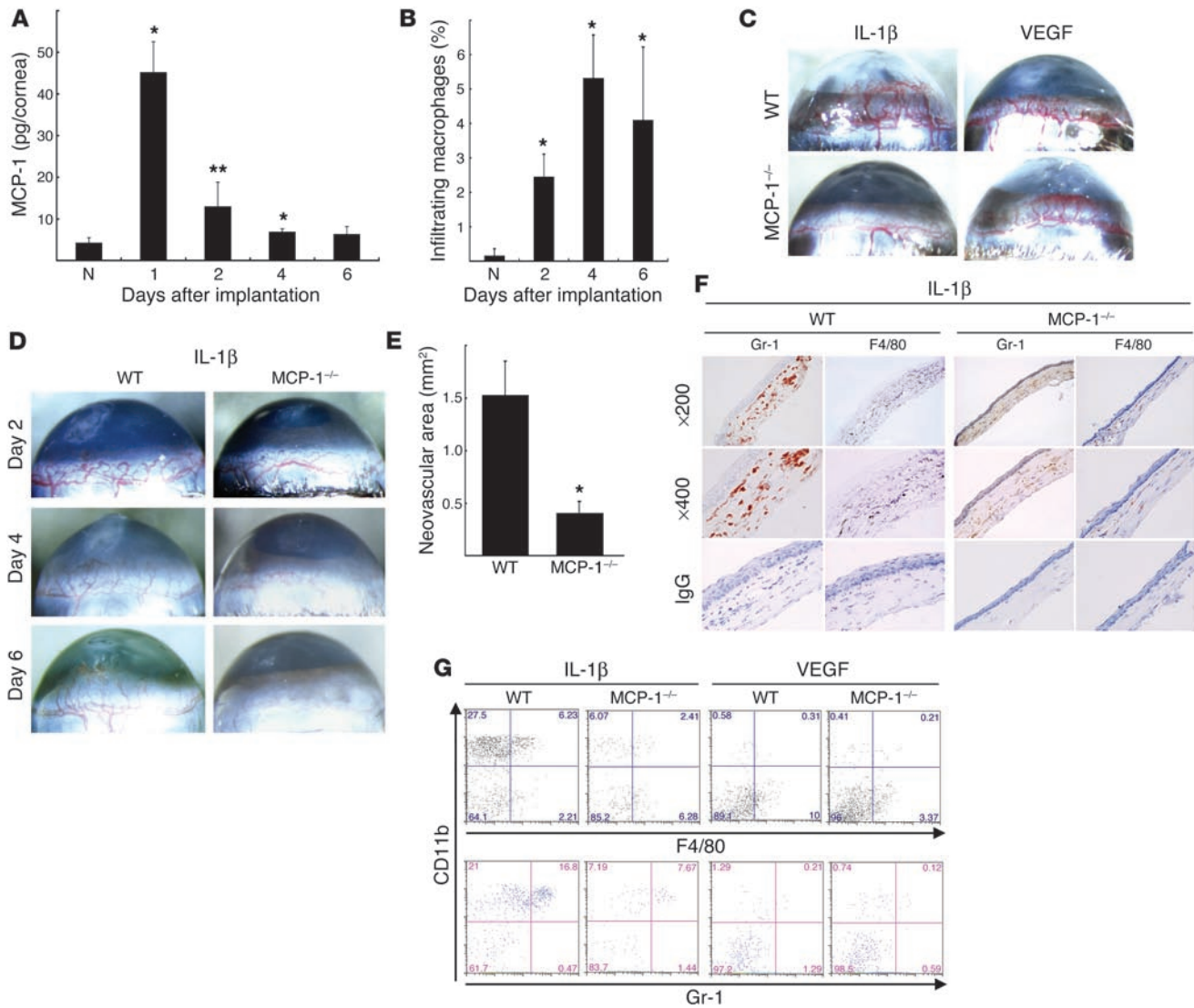


**Figure 3**

The role of MCP-1 in IL-1 $\beta$ - or VEGF-induced angiogenesis. **(A)** Kinetics of MCP-1 levels after pellet implantation. Corneal lysates were prepared and assayed by ELISA at the indicated times ( $n = 3$ ). \* $P < 0.01$  and \*\* $P < 0.03$  versus untreated (N). **(B)** Kinetics of infiltrating macrophages in IL-1 $\beta$ -implanted corneas. Corneal lysates were prepared from untreated and IL-1 $\beta$ -treated corneas on the days shown ( $n = 3$ ). Percentages of infiltrating F4/80 $^{+}$  cells were quantified using FACS. **(C)** Corneal neovascularization induced by IL-1 $\beta$  (30 ng) or VEGF (200 ng) in C57BL/6 wild-type and MCP-1 $^{-/-}$  mice on day 6. **(D)** Corneal neovascularization at the indicated time points. **(E)** Quantitative analysis of IL-1 $\beta$ -induced corneal neovascularization in MCP-1 $^{-/-}$  ( $n = 10$ ) and wild-type mice ( $n = 8$ ) on day 6. Bars show means  $\pm$  SD. \* $P < 0.01$  versus wild-type mice using the unpaired Student's  $t$  test. **(F)** Immunohistochemistry for Gr-1 or F4/80 (brown) in corneal sections on day 6 after IL-1 $\beta$  pellet implantation in MCP-1 $^{-/-}$  or wild-type mice. Gr-1-positive cells were detected in both types of mice. F4/80-positive cells were detected on day 6 in wild-type but not MCP-1 $^{-/-}$  mice. **(G)** FACS analysis of infiltrating cells from 5 IL-1 $\beta$ - or VEGF-implanted corneas at day 6 in wild-type or MCP-1 $^{-/-}$  mice. The percentages of CD11b $^{+}$ F4/80 $^{+}$  cells were 4.09%  $\pm$  2.13% (IL-1 $\beta$ , wild-type), 2.53%  $\pm$  1.73% (IL-1 $\beta$ , MCP-1 $^{-/-}$ ), 0.30%  $\pm$  0.10% (VEGF, wild-type), and 0.14%  $\pm$  0.05% (VEGF, MCP-1 $^{-/-}$ ). The percentages of CD11b $^{+}$ Gr-1 $^{+}$  cells were 13.5%  $\pm$  2.89% (IL-1 $\beta$ , wild-type), 7.84%  $\pm$  0.48% (IL-1 $\beta$ , MCP-1 $^{-/-}$ ), 0.94%  $\pm$  0.55% (VEGF, wild-type) and 0.20%  $\pm$  0.10% (VEGF, MCP-1 $^{-/-}$ ).

(anti-Gr-1) and macrophages (anti-F4/80). On day 2, the infiltrate mainly contained neutrophils (Figure 1E) with some F4/80-positive macrophages. On day 6, numerous F4/80-positive macrophages were detected. Flow cytometry revealed that Gr-1-positive neutrophils were abundant on day 2 (53.5%  $\pm$  10.4%) but decreased on days 4 (15.8%  $\pm$  4.9%) and 6 (3.15%  $\pm$  0.27%). In contrast, F4/80-positive macrophages increased on days 4 (5.56%  $\pm$  1.61%) and 6 (5.52%  $\pm$  1.14%). There was minimal neutrophil and macrophage infiltration of control corneas implanted with hydon pellets alone

(Figure 1F). There were 2- to 3-fold increases in the number of infiltrating macrophages 4 and 6 days after VEGF treatment compared with the untreated control. IL-1 $\beta$  induced the early infiltration of neutrophils, followed by macrophages, during angiogenesis. VEGF had weaker effects on neutrophil and macrophage infiltration.

*Effect of neutrophil depletion on IL-1 $\beta$ -induced angiogenesis.* Neutrophils were depleted by i.p.-administered anti-Gr-1 Ab in order to determine their roles in IL-1 $\beta$ - and VEGF-induced angiogenesis. Reduced numbers of polymorphic mononuclear cells were seen

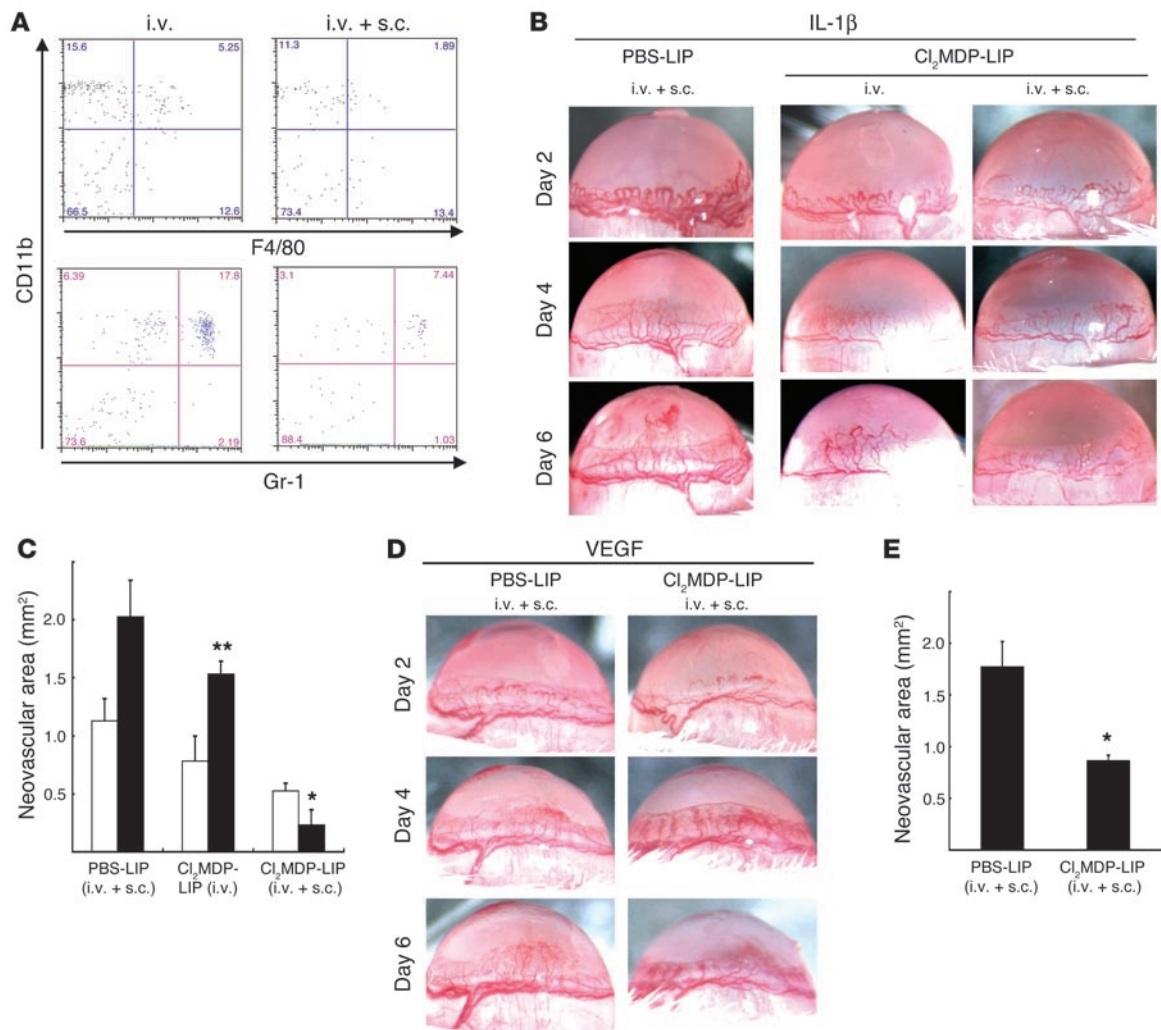


**Figure 4** The effect of Cl<sub>2</sub>MDP-LIPs on IL-1β-induced angiogenesis. **(A)** FACS analysis of infiltrating cells on day 6, in IL-1β-implanted corneas from BALB/c mice that received Cl<sub>2</sub>MDP-LIPs or PBS-LIPs i.v. and/or s.c. The cells were stained with PE-CD11b mAb and FITC-Gr-1 or FITC-F4/80 mAb. **(B)** Corneal neovascularization at the indicated time points in BALB/c mice receiving Cl<sub>2</sub>MDP-LIPs or PBS-LIPs i.v. and/or s.c. The percentages of infiltrating cells in IL-1β-implanted corneas of Cl<sub>2</sub>MDP-LIP- or PBS-LIP-treated mice were 4.75% ± 0.48% (i.v., CD11b<sup>+</sup>F4/80<sup>+</sup>), 13.2% ± 4.03% (i.v., CD11b<sup>+</sup>Gr-1<sup>+</sup>), 1.63% ± 0.30% (i.v. + s.c., CD11b<sup>+</sup>F4/80<sup>+</sup>), and 6.61% ± 0.93% (i.v. + s.c., CD11b<sup>+</sup>Gr-1<sup>+</sup>). **(C)** Neovascularization was quantified by area in mm<sup>2</sup> on day 4 (white bars) and day 6 (black bars). Bars show means ± SD of independent experiments (n = 3 or 4; \*P < 0.01 and \*\*P < 0.05 versus PBS-LIPs). **(D)** Corneal neovascularization induced with VEGF at the indicated time points after receiving Cl<sub>2</sub>MDP-LIPs or PBS-LIPs (i.v. + s.c.). **(E)** Quantitative analysis of neovascularization on day 6. VEGF-induced corneal neovascularization in mice (n = 6) receiving Cl<sub>2</sub>MDP-LIPs was inhibited compared with mice (n = 6) receiving PBS-LIPs. \*P < 0.01 using the Student's t test.

in the peripheral blood 6 days after treatment (data not shown). Neither IL-1β- nor VEGF-induced angiogenesis was influenced by neutrophil depletion by anti-Gr-1 Ab (Figure 2, A and B). No cell infiltration was detected in IL-1β-implanted corneas treated with anti-Gr-1 Ab although edema was observed on day 2 (Figure 2C). The CD11b<sup>+</sup>Gr-1<sup>+</sup> cell population was reduced by 99.5% after 2 days whereas CD11b<sup>+</sup>Gr-1<sup>-</sup> and CD11b<sup>+</sup>F4/80<sup>+</sup> cells persisted (Figure 2, D and E). Anti-Gr-1 Ab did not affect the appearance of F4/80-positive macrophages, suggesting neutrophil infiltration was not required for IL-1β-induced angiogenesis in mouse corneas.

*IL-1β-induced angiogenesis in MCP-1<sup>-/-</sup> mouse corneas.* The CC chemokine MCP-1 is a potent macrophage chemoattractant (12). MCP-1<sup>-/-</sup> mice show reduced macrophage recruitment to

inflammatory sites (13–15). MCP-1 is induced by IL-1β in vitro (32), but its role in angiogenesis in vivo is unclear. ELISA showed that MCP-1 levels were significantly increased 1 day after IL-1β implantation, remained high on day 2, and were similar to those in untreated corneas on day 6 (Figure 3A). The macrophage infiltration of the IL-1β-treated corneas increased over time and peaked on day 4 (Figure 3B).

In MCP-1<sup>-/-</sup> mice, implanting VEGF pellets induced corneal neovascularization at levels similar to those of C57BL/6 wild-type mice (Figure 3C). In contrast, IL-1β-induced angiogenesis was reduced in MCP-1<sup>-/-</sup> compared with wild-type mice (Figure 3, C and D). Quantitative analysis demonstrated less IL-1β-induced corneal neovascularization in MCP-1<sup>-/-</sup> mice than in C57BL/6



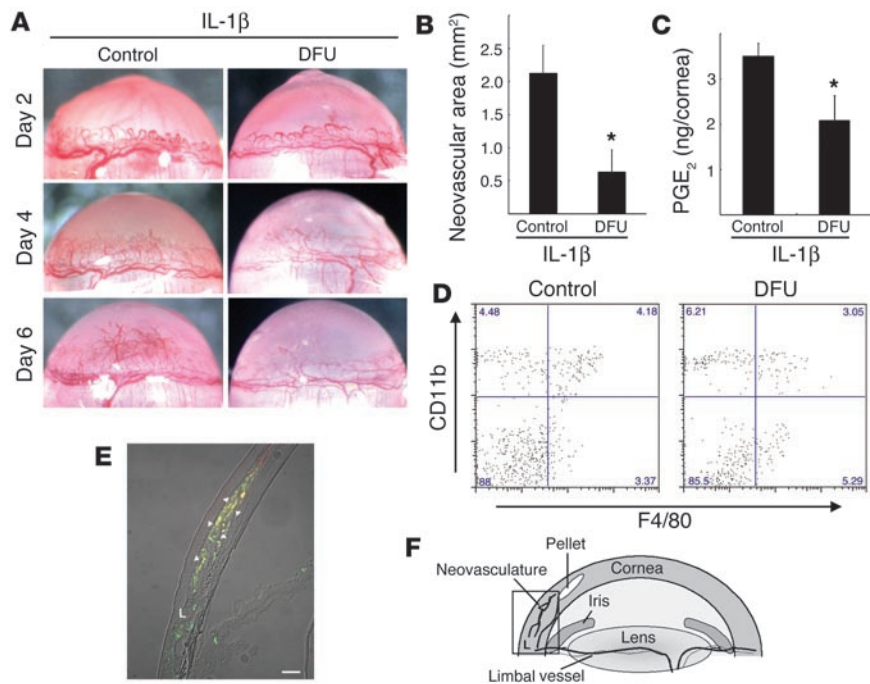


**Figure 5** Expression of COX-2 in infiltrating macrophages during IL-1 $\beta$ -induced angiogenesis. **(A)** Corneal neovascularization on days 2, 4, and 6 in BALB/c mice receiving DFU. **(B)** Quantitative analysis of neovascularization on day 6. IL-1 $\beta$ -induced corneal neovascularization in mice ( $n = 5$ ) receiving DFU was inhibited compared with control mice ( $n = 7$ ). \* $P < 0.01$  using Student's  $t$  test. **(C)** Comparison of levels of PGE $_2$  in IL-1 $\beta$ -implanted corneas with or without DFU. On day 4, 4 IL-1 $\beta$ -implanted corneas of DFU-treated and untreated mice were harvested. Corneal lysates were prepared and individually assayed for PGE $_2$  ( $n = 3$ ). \*\* $P < 0.05$  using Student's  $t$  test. **(D)** FACS analysis of infiltrating cells on day 6 from 5 IL-1 $\beta$ -implanted corneas from BALB/c mice receiving DFU and control mice. The percentages of CD11b $^+$ F4/80 $^+$  cells in mouse corneas were 4.63%  $\pm$  0.52% (control) and 3.45%  $\pm$  0.57% (DFU treated). **(E)** Representative overview of an IL-1 $\beta$ -implanted cornea on day 4. Arrowheads indicate infiltrated cells (yellow) that are positive for macrophage marker F4/80 (green) and COX-2 (red). L, limbus. Scale bar: 50  $\mu$ m. **(F)** Corneal micropocket assay model in mice. The rectangle represents the area of the cornea used in the immunohistochemical analysis in **E**.

wild-type mice (Figure 3E). Vascular loops and sprouts typical of corneal neovascularization were present in C57BL/6 and BALB/c mice (Figures 1B and 3D). On day 2 after IL-1 $\beta$  treatment, vascular loops were seen in the neovasculature of MCP-1 $^{-/-}$  mice. On days 4 and 6, the vessel sprouts were reduced in MCP-1 $^{-/-}$  mice compared with wild-type mice. The infiltration of Gr-1-positive neutrophils into IL-1 $\beta$ -treated corneas of wild-type and MCP-1 $^{-/-}$  mice was confirmed histologically and by flow cytometry (Figure 3, F and G). The number of Gr-1-positive neutrophils was lower in MCP-1 $^{-/-}$  mice than in wild-type mice. There was less infiltration by F4/80-positive macrophages in IL-1 $\beta$ -treated MCP-1 $^{-/-}$  mice than in IL-1 $\beta$ -treated wild-type mice, suggesting an important role for these cells in IL-1 $\beta$ -induced corneal neovascularization.

**Macrophage depletion reduced IL-1 $\beta$ -induced angiogenesis.** Clodronate liposomes (Cl $_2$ MDP-LIPs) are phagocytosed by macrophages and induce rapid apoptosis (33, 34). Cl $_2$ MDP-LIPs administered i.v. to mice depleted macrophages in the spleen and liver (data not shown) but not the cornea (Figure 4A) and mildly inhibited IL-1 $\beta$ -induced angiogenesis (Figure 4, B and C). Cl $_2$ MDP-LIPs administered by i.v. and subconjunctival (s.c.) injection depleted macrophages in the cornea (80.5% depletion on day 6), spleen, liver,

and submandibular lymph nodes (Figure 4, B and C). This treatment did not affect the IL-1 $\beta$ -induced corneal vascular loops on day 2. However, weak vascular sprouts, compared with those in controls, were observed on day 4, and a reduction in corneal neovascularization was detected on day 6. Control PBS-containing liposomes (PBS-LIPs) did not affect IL-1 $\beta$ -induced corneal neovascularization. Quantitative analysis demonstrated that Cl $_2$ MDP-LIP treatment (i.v. and s.c.) significantly reduced IL-1 $\beta$ -induced corneal neovascularization (Figure 4, B and C) and angiogenesis on day 6. PBS-LIP treatment had no effect on VEGF-induced angiogenesis while Cl $_2$ MDP-LIP treatment (i.v. and s.c.) inhibited VEGF-induced corneal neovascularization by approximately 50% compared with the control on day 6 (Figure 4, D and E).

**IL-1 $\beta$ -induced angiogenesis and the infiltration of monocytes/macrophages expressing COX-2.** COX-2 inhibitors block IL-1 $\beta$ - but not VEGF-induced angiogenesis (31). COX-2 $^{-/-}$  mice lack IL-1 $\beta$ -induced corneal angiogenesis whereas VEGF-induced angiogenesis is not affected, suggesting that COX-2 is involved in the former (31). IL-1 $\beta$ -induced angiogenesis on days 4 and 6 was blocked by oral administration of a selective COX-2 inhibitor, 5,5-dimethyl-3-(3-fluorophenyl)-4-(4-methylsulphonyl)phenyl-2((5H)-furanone (DFU) (Figure 5, A and B). On day 4, administration of DFU reduced levels of PGE $_2$ , a main product of COX-2, in corneas by 41% of that in untreated control (Figure 5C).

CD11b $^+$ F4/80 $^+$  cells infiltrated the corneas of DFU-treated mice (Figure 5D), suggesting that COX-2 inhibition did not influence macrophage infiltration. Immunostaining with mAb F4/80 showed the infiltration of monocyte/macrophage-like cells around the neovasculature on day 4 induced by IL-1 $\beta$  (Figure 5E). F4/80-positive macrophages near the limbal vessel were COX-2 negative whereas those that infiltrated more deeply were COX-2 positive (Figure 5E). Thus, only activated macrophages expressed COX-2. There was no macrophage infiltration into the control corneas (data not shown).

**MCP-1 in tumor growth and angiogenesis in cancer cells expressing IL-1 $\beta$ .** We compared angiogenesis induced by Lewis lung carcinoma cells expressing IL-1 $\beta$  (LLC/IL-1 $\beta$ ) and LLC cells expressing neo<sup>R</sup> (LLC/neo) cells in a dorsal air sac assay in wild-type C57BL/6 and MCP-1 $^{-/-}$  mice. Serum levels of MCP-1 and IL-1 $\beta$  were measured 7 days after inoculation with LLC/neo and LLC/IL-1 $\beta$  cells using ELISAs (Figure 6A and 6B). MCP-1 was not detected in LLC/neo-grafted or control ungrafted mice. In LLC/IL-1 $\beta$ -grafted wild-type mice, the serum MCP-1 concentration was 40.8  $\pm$  5.31 pg/ml compared with 3.43  $\pm$  0.56 pg/ml in LLC/IL-1 $\beta$ -grafted MCP-1 $^{-/-}$  mice (Figure 6A). There were similar serum IL-1 $\beta$  levels in LLC/IL-1 $\beta$ -grafted wild-type and MCP-1 $^{-/-}$  mice (334  $\pm$  104 and 302  $\pm$  124 pg/ml, respectively; Figure 6B). LLC/neo and LLC/IL-1 $\beta$

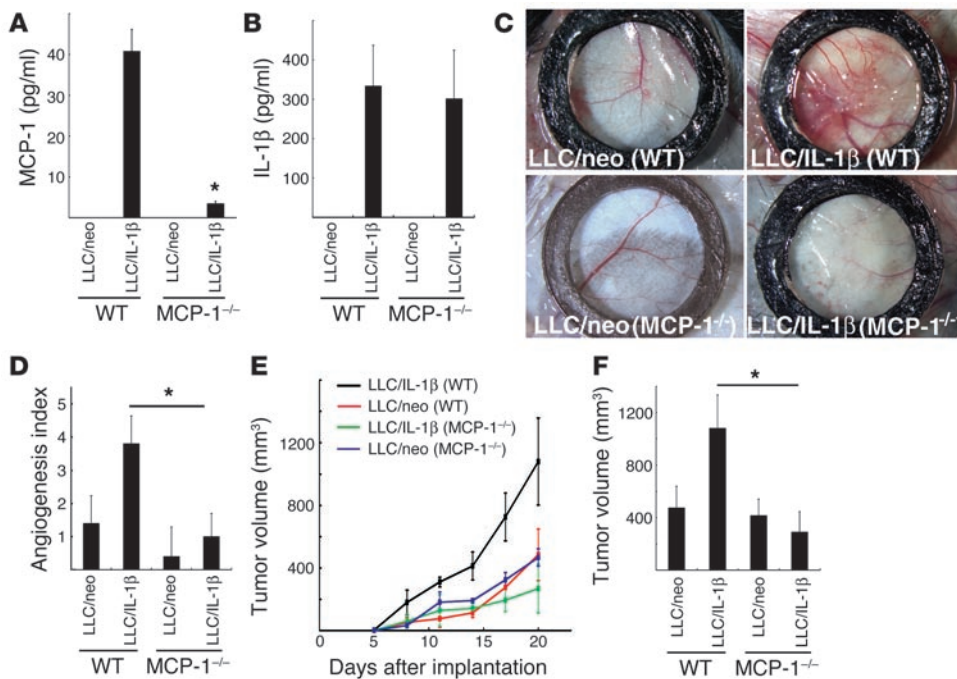


**Figure 6** IL-1β-induced tumor angiogenesis in MCP-1<sup>-/-</sup> mice. (A) MCP-1 levels in the serum of LLC/IL-1β-grafted MCP-1<sup>-/-</sup> mice and wild-type mice 7 days after inoculation. MCP-1 was not detectable in the serum of LLC/neo-grafted mice by ELISA. Values are expressed as means ± SD of 5 samples. (B) IL-1β levels in the serum of LLC/IL-1β-grafted MCP-1<sup>-/-</sup> mice compared with wild-type mice 7 days after inoculation. \*P < 0.01 using the unpaired Student's *t* test. Values are expressed as means ± SD (*n* = 5). (C) Representative photographs of the dorsal air sac assay with LLC/neo and LLC/IL-1β in C57BL/6 wild-type and MCP-1<sup>-/-</sup> mice. (D) Quantitative analysis of the neovascularization induced by LLC/neo or LLC/IL-1β in the dorsal air sac in wild-type and MCP-1<sup>-/-</sup> mice. Mean angiogenetic activities ± SD for groups of mice (*n* = 5). \*P < 0.01 versus LLC/IL-1β using the Mann-Whitney *U* test. (E) Mean tumor volumes ± SD for groups of wild-type mice (black and red) or MCP-1<sup>-/-</sup> mice (green and blue) implanted with 5 × 10<sup>5</sup> LLC/IL-1β or LLC/neo cells (*n* = 5). (F) LLC/IL-1β tumor growth was not enhanced in MCP-1<sup>-/-</sup> mice (*n* = 10) compared with wild-type mice (*n* = 10; day 20). \*P < 0.01 using the unpaired Student's *t* test.

cells showed identical growth rates in culture (6). IL-1β and MCP-1 are thus unlikely to promote the proliferation of LLC cells.

Implanting a chamber containing LLC/IL-1β into C57BL/6 wild-type mice produced curled microvessels and numerous tiny bleeding spots (Figure 6C). The implantation of chambers containing LLC/IL-1β into MCP-1<sup>-/-</sup> C57BL/6 mice produced less neovascularization than in wild-type mice. In contrast, less neovascularization was seen when LLC/neo was implanted into wild-type mice (Figure 6C). Quantitative analyses revealed 3-fold greater neovascular development induced by LLC/IL-1β compared with LLC/neo in wild-type mice. However, implanting LLC/IL-1β into MCP-1<sup>-/-</sup> mice markedly reduced angiogenesis (Figure 6D).

Grafting LLC/neo or LLC/IL-1β cells into C57BL/6 wild-type and MCP-1<sup>-/-</sup> mice confirmed that the latter grew faster than the former in wild-type mice (Figure 6E). LLC/IL-1β-grafted tumors in MCP-1<sup>-/-</sup> mice were significantly smaller than in wild-type mice. There was no difference in LLC/neo tumor growth between MCP-1<sup>-/-</sup> and wild-type mice (Figure 6, E and F).

Selective staining of endothelial cells showed a reduction of microvascular density of approximately 50% in LLC/IL-1β tumors grafted into MCP-1<sup>-/-</sup> mice compared with LLC/IL-1β tumors in wild-type mice (Figure 7, A and B). Immunostaining using mAb F4/80 revealed fewer macrophages in LLC/IL-1β tumors from

MCP-1<sup>-/-</sup> mice. However, there were similar numbers of infiltrating macrophages in LLC/neo tumors in wild-type and MCP-1<sup>-/-</sup> mice. Quantitative analysis revealed more F4/80-positive infiltrating macrophages in LLC/IL-1β tumors than in LLC/neo tumors (Figure 7, C and D). The number of macrophages was lower in LLC/IL-1β tumors in MCP-1<sup>-/-</sup> mice than in wild-type mice. It remains unclear why there were more infiltrating macrophages in LLC/neo than in LLC/IL-1β tumors, as the microvascular density was similar in both (Figure 7, B and D).

*COX-2 in angiogenesis, tumor growth, and macrophage infiltration in cancer cells expressing IL-1β.* Implanting a chamber containing LLC/IL-1β led to the development of microvessels (Figure 8A) while oral administration of a COX-2 inhibitor reduced this activity. Quantitative analyses revealed 3-fold greater development of the neovasculture induced by LLC/IL-1β compared with LLC/neo. Treatment with a COX-2 inhibitor significantly reduced the angiogenesis induced by LLC/IL-1β (Figure 8B).

Both LLC/IL-1β- and LLC/neo-tumor growth were inhibited by treatment with DFU, although the former was more strongly affected (Figure 8, C and D). Selective

staining of endothelial cells showed the microvascular density was increased approximately 1.5-fold in LLC/IL-1β tumors compared with LLC/neo tumors grafted into mice. DFU reduced the microvascular density in LLC/IL-1β tumors but was less effective in LLC/neo tumors (Figure 8, E and F). Immunostaining revealed fewer macrophages in LLC/IL-1β tumors in DFU-treated mice compared with control mice (Figure 8G). However, there were similar numbers of infiltrating macrophages in LLC/neo tumors in control and DFU-treated mice. Quantitative analysis revealed fewer F4/80-positive infiltrating macrophages in DFU-treated LLC/IL-1β tumors compared with control tumors (Figure 8H).

*Partial involvement of ELR<sup>+</sup> chemokines in IL-1β-induced angiogenesis.* CXC chemokines containing the ELR motif (ELR<sup>+</sup>), including IL-8, growth-related oncogenes (GRO) α, β, and γ (CXC chemokine ligand 1 [CXCL1], CXCL2, and CXCL3), and epithelial neutrophil-activating peptide-78 (ENA-78 or CXCL5), potentially induce angiogenesis (35). This activity is mediated by CXC chemokine receptor 2 (CXCR2; ref. 36). Anti-CXCR2 Abs inhibited the growth of LLC/IL-1β cells in vivo (6).

We examined the levels of various ELR<sup>+</sup> CXC chemokines, including KC (CXCL1), macrophage inflammatory protein 2 (MIP-2, also known as CXCL2/3), and VEGF-A, in IL-1β-implanted corneas using ELISA. KC, MIP-2, and VEGF-A were elevated 2 days after



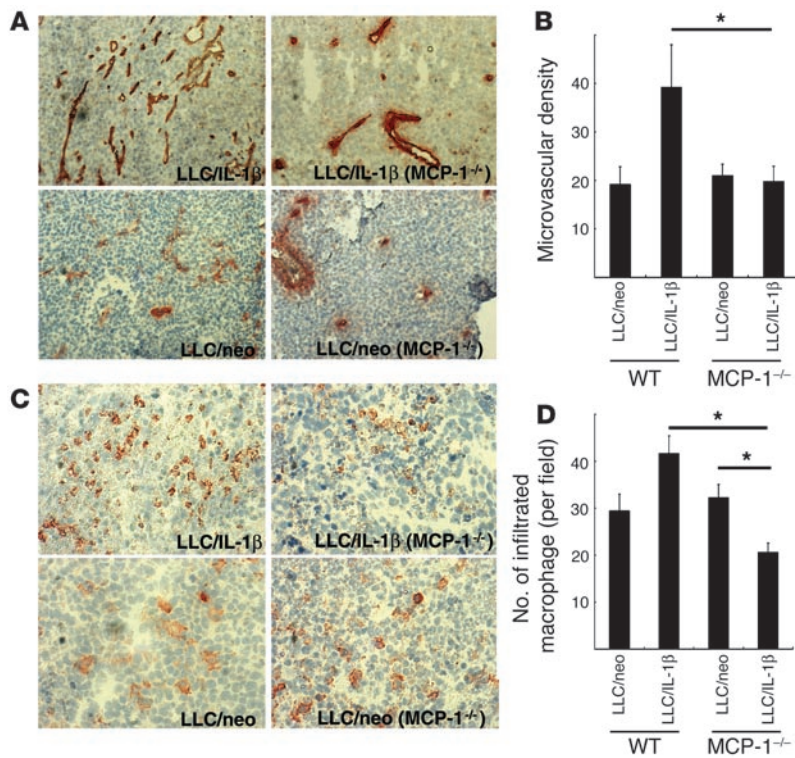


**Figure 7**

Enhancement of angiogenesis and macrophage infiltration by LLC/IL-1β was inhibited in MCP-1<sup>-/-</sup> mice (A) Representative photographs of CD31-stained sections from LLC tumors in wild-type or MCP-1<sup>-/-</sup> mice. Magnification, ×400. (B) CD31-positive microvascular densities obtained by morphometric analysis of LLC tumors. Each value represents the mean number of vessels ± SD in 5 fields. \*P < 0.01 versus LLC/IL-1β. (C) Infiltration of macrophages stained with mAb F4/80 in LLC/neo and LLC/IL-1β tumors. Magnification, ×200. (D) Quantification of the number of macrophages infiltrating LLC/IL-1β and LLC/neo tumors. Magnification, ×400. Each value represents the mean number of macrophages ± SD in 5 microscopic fields. \*P < 0.01 versus LLC/IL-1β in wild-type mice using the Mann-Whitney U test.

implantation (Figure 9, A–C). ENA-78 (CXCL5) mRNA levels were also increased in IL-1β-implanted corneas compared with controls (Figure 9D). Anti-mouse CXCR2 Ab inhibited IL-1β-implanted corneal angiogenesis by 32% (Figure 9, E and F).

CXC chemokines and VEGF-A are involved in COX-2-associated angiogenesis (37, 38). VEGF-A and KC levels were decreased in the IL-1β-implanted corneas of DFU-treated mice compared with control mice (Figure 9, G and H). ELR<sup>+</sup> CXC chemokine–CXCR2 signaling was therefore important for COX-2-related angiogenesis induced by IL-1β.

**Discussion**

IL-1 has been implicated in the growth of solid tumors, hematopoiesis, leukemia, and atherosclerosis (3). IL-1β is overexpressed in ovarian cancer cells in culture (39) and in patients with renal cell and gastric cancers (40, 41); it is essential for inflammatory and tumor-associated angiogenesis in animal models (6–8). Reduced angiogenesis and tumor enlargement have been reported in IL-1β-KO mice (8, 10). Various angiogenesis-related factors are upregulated by IL-1β overexpression when human lung cancer cells are transplanted into animals (7). Bar et al. reported that IL-1 receptor antagonist inhibited IL-1β-transfected tumor proliferation in an in vivo xenograft model (9).

Tumors expressing IL-1β are characterized by the infiltration of neutrophils, lymphocytes, and macrophages (9). However, it has been unclear which was most important in IL-1β-induced angiogenesis. We used 2 assays to confirm that IL-1β-induced angiogenesis was suppressed in mouse corneas by monocyte/macrophage depletion. First, Cl<sub>2</sub>MDP-LIPs (i.v. and s.c.) blocked monocyte/macrophage infiltration and IL-1β-induced angiogenesis, depleting macrophages but not neutrophils or lymphocytes (33, 34). Second, neovascularization and the numbers of infiltrat-

ing macrophages were reduced in MCP-1<sup>-/-</sup> mice given IL-1β-containing corneal implants. MCP-1 acts potently on mononuclear cells, including monocytes and lymphocytes. MCP-1<sup>-/-</sup> mice have shown impaired macrophage recruitment in several inflammatory models in vivo (13–15). Neutrophil depletion by anti-Gr-1 mAb did not affect IL-1β-induced corneal angiogenesis. These results suggest that the infiltration of monocytes/macrophages rather than neutrophils is crucial in IL-1β-induced angiogenesis.

Conejo-Garcia et al. (42) reported that angiogenesis induced by infiltrating dendritic cell precursors was mediated through the cooperation of β-defensins and VEGF-A, suggesting the involvement of immune mechanisms in tumor angiogenesis (42). The role of dendritic cell infiltration in IL-1β-induced angiogenesis and the effect of Cl<sub>2</sub>MDP-LIPs on dendritic cells have been unclear. Zhang et al. (43) reported that Cl<sub>2</sub>MDP-LIPs depleted CD11c-positive dendritic cells in the spleen but not in peripheral blood. Cheng et al. (44) demonstrated that s.c. injection of Cl<sub>2</sub>MDP-LIPs depleted macrophages but not dendritic cells. We found that CD11c<sup>+</sup> dendritic cells were 1.4% ± 0.5% (PBS-LIP treatment) and 1.3% ± 0.4% (Cl<sub>2</sub>MDP-LIP treatment), respectively, of total cells in peripheral blood when Cl<sub>2</sub>MDP-LIPs were administered both i.v. and s.c. (n = 5; Supplemental Figure S1; supplemental material available online with this article; doi:10.1172/JCI23298DS1). The numbers of infiltrating CD11c<sup>+</sup> dendritic cells in IL-1β-treated corneas were similar in Cl<sub>2</sub>MDP-LIP- and PBS-LIP-treated mice (Supplemental Figure S2). IL-1β-induced angiogenesis was blocked in MCP-1<sup>-/-</sup> mice (Figure 3), and dendritic cells did not express the CCR2 cognate receptor for MCP-1. Thus, infiltrating dendritic cells are unlikely to be important in neovascularization mediated by IL-1β.

Maximum MCP-1 expression occurred 1 day after IL-1β implantation into mouse corneas (Figure 3). MCP-1 is essential in the recruitment of angiogenic macrophages (12, 16). In wild-type



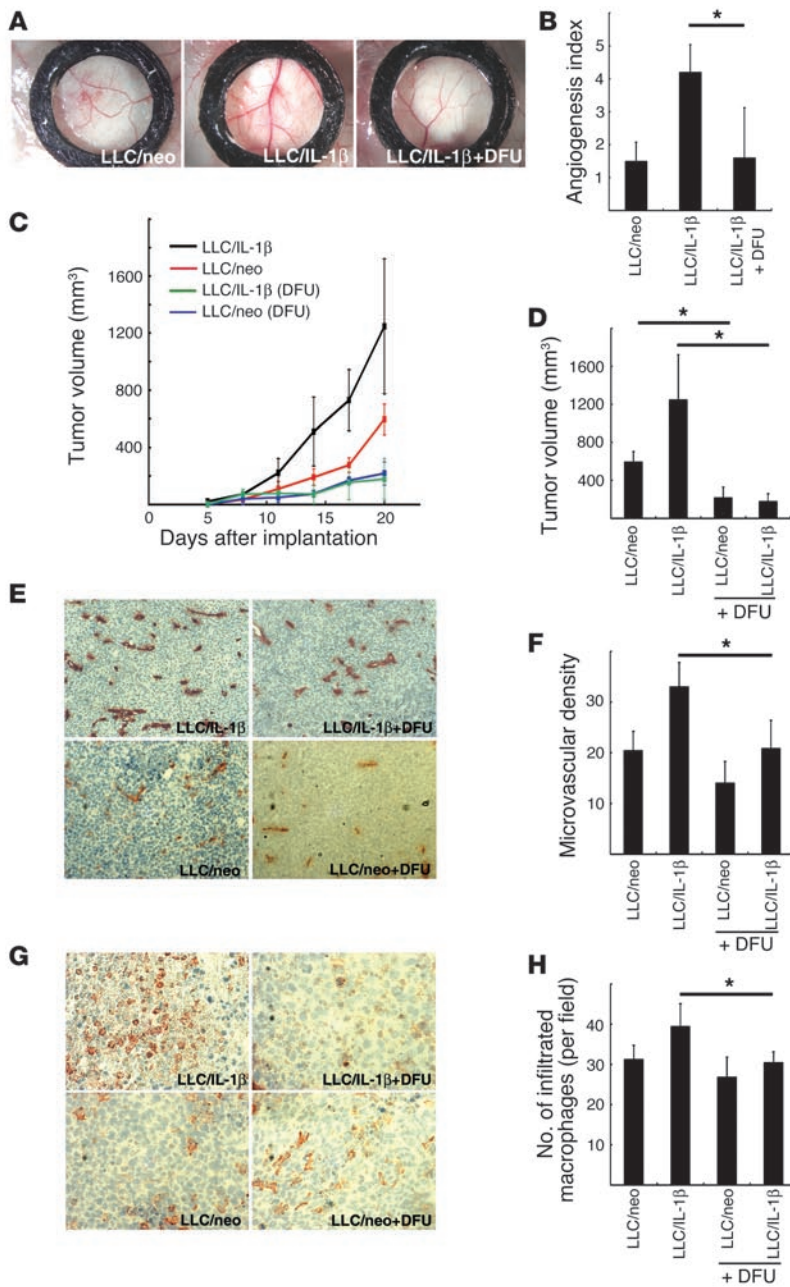


**Figure 8**

The effect of a COX-2 inhibitor on IL-1 $\beta$ -induced tumor angiogenesis. (A) Representative photographs of dorsal air sac assays in BALB/c mice with LLC/neo and LLC/IL-1 $\beta$  untreated or treated with DFU. (B) Quantitative analysis of the neovascularization induced by LLC/neo or LLC/IL-1 $\beta$  in the dorsal air sac assay in mice untreated or treated with DFU. Mean angiogenesis activities  $\pm$  SD for groups of mice ( $n = 5$ ). \* $P < 0.01$  versus LLC/IL-1 $\beta$ . (C) Tumor volumes in wild-type mice implanted with  $5 \times 10^5$  LLC/IL-1 $\beta$  or LLC/neo cells, untreated or treated with DFU. (D) LLC/IL-1 $\beta$  and LLC/neo tumor growth was inhibited in DFU-treated mice compared with control mice (day 20). \* $P < 0.01$  using unpaired Student's  $t$  test. (E) Representative photographs of CD31-stained tumor sections from LLC tumors grown in wild-type mice. Magnification,  $\times 400$ . (F) CD31-positive microvascular densities from morphometric analysis of LLC tumors. Each value represents the mean number of vessels  $\pm$  SD in 5 fields. \* $P < 0.01$ . (G) Infiltration of macrophages stained with mAb F4/80 in LLC/neo and LLC/IL-1 $\beta$  tumors in the mice indicated. Magnification,  $\times 200$ . (H) Quantification of macrophages infiltrating LLC/IL-1 $\beta$  and LLC/neo tumors under the microscope. Magnification,  $\times 400$ . Each value represents the mean number of macrophages  $\pm$  SD in 5 fields. \* $P < 0.01$  versus LLC/IL-1 $\beta$  wild-type mice using the Mann-Whitney  $U$  test.

present on days 4 or 6 (Figure 3D). The appearance of dilated loop structures might not directly affect angiogenesis, and the underlying mechanism remains unclear. Cl<sub>2</sub>MDP-LIPs reduced the appearance of IL-1 $\beta$ -induced vascular sprouts compared with controls on day 4 and decreased the corneal neovascularization on day 6. Macrophages might therefore be important for the sprouting and maintenance of IL-1 $\beta$ -induced neovascularization.

IL-1 $\beta$  reportedly induced MCP-1 expression in endothelial cells (32). We observed increased MCP-1 levels in the serum of LLC/IL-1 $\beta$ -grafted wild-type mice compared with LLC/neo-grafted wild-type mice (Figure 6). Only a slight increase in MCP-1 was observed in LLC/IL-1 $\beta$ -grafted MCP-1<sup>-/-</sup> mice. MCP-1 expression is reportedly associated with macrophage accumulation in various human cancers (46). Here we demonstrated that IL-1 $\beta$ - but not VEGF-induced corneal neovascularization was inhibited in

mice, F4/80<sup>+</sup> macrophage infiltration into IL-1 $\beta$ -implanted corneas was observed after day 4. The number of infiltrating macrophages increased 2 days after IL-1 $\beta$  treatment and peaked on day 4. We previously demonstrated maximum levels of MIP-1 $\alpha$  (a potent chemoattractant) and VEGF in mouse corneas 0.5–1 days after cauterization by silver nitrate. The infiltration of macrophages peaked on day 3, and neovascularization peaked on day 5 (45). These results suggest that the expression of potent attractants (such as MCP-1 and MIP-1 $\alpha$ ) 0.5–1 days after the presentation of inflammatory stimuli influences the subsequent appearance of macrophages. Determining the causative link between these processes in vivo will require further studies.

On day 2, dilated vascular loop structures were observed in MCP-1<sup>-/-</sup> and wild-type mice whereas vessel sprouts were not

MCP-1<sup>-/-</sup> mice. Moreover, LLC/IL-1 $\beta$  but not LLC/neo tumor growth was inhibited. Macrophage infiltration in IL-1 $\beta$ -implanted corneas and LLC/IL-1 $\beta$  tumor growth were impaired in MCP-1<sup>-/-</sup> mice compared with wild-type mice. Thus, the IL-1 $\beta$ -induced recruitment of angiogenic macrophages depended upon the upregulation of MCP-1 in vivo. MCP-1 appears to be pivotal in proinflammatory cytokine-induced angiogenesis and tumor growth, possibly through enhancing macrophage infiltration (Figure 10).

Lu et al. reported similar hematologic profiles in MCP-1<sup>-/-</sup> and wild-type mice (13). Low et al. demonstrated that MCP-1<sup>-/-</sup> leukocytes proliferated normally when stimulated in vitro (15). Freshly isolated monocytes from healthy donors expressed CCR2, but MCP-1 suppressed this during their differentiation into macrophages in vitro (47). The number of infiltrating macrophages in

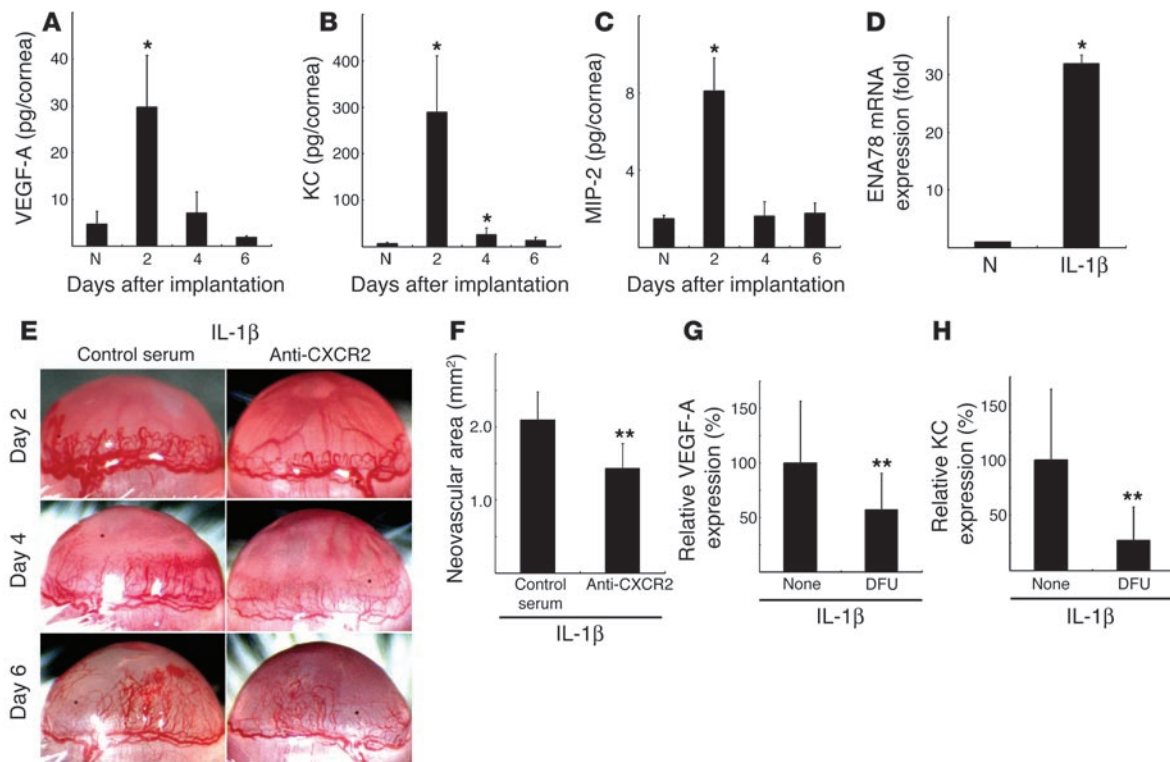


**Figure 9** The effect of anti-CXCR2 Ab on IL-1β–induced angiogenesis. Kinetics of protein expression for (A) VEGF-A, (B) KC (mouse CXCL1), and (C) MIP-2 (mouse CXCL2/3) after IL-1β pellet implantation. Four corneal lysates were prepared and assayed by ELISA on the indicated days (*n* = 3). \**P* < 0.01 versus untreated. (D) Expression of ENA-78 (CXCL5) mRNA levels in IL-1β–treated corneas. Six IL-1β–implanted corneas (IL-1β) or untreated corneas (N) were harvested, and real-time RT-PCR was performed to determine ENA-78 (CXCL5) mRNA levels on day 2. Expression was normalized to GAPDH mRNA levels. \**P* < 0.01 versus untreated. (E) Corneal neovascularization on days 2, 4, and 6 in BALB/c mice with or without i.p. administration of anti-mouse CXCR2 Ab. (F) Quantitative analysis of neovascularization on day 6. IL-1β–induced corneal neovascularization in mice (*n* = 6) receiving anti-mouse CXCR2 Ab was inhibited compared with mice (*n* = 6) receiving control goat serum. \*\**P* < 0.05 using Student’s *t* test. (G and H) Comparison of levels of VEGF-A (G) and KC (H) in IL-1β–implanted corneas with or without DFU. On day 4, corneal lysates were prepared from 4 IL-1β–implanted corneas from DFU-treated and untreated mice and individually assayed by ELISA for VEGF-A or KC (*n* = 3). \*\**P* < 0.05 using Student’s *t* test.

MCP-1<sup>-/-</sup> mice was lower compared with wild-type mice after IL-1β treatment. MCP-1 deficiency might affect both macrophage recruitment and differentiation. Further studies will be required to establish the role of MCP-1 in macrophage differentiation.

Lyden et al. (48) reported the infiltration of Flt-1–positive monocytes in LLC-induced tumors. Anti-Flt-1 Ab inhibited their growth, suggesting that VEGF might promote monocyte/macrophage infiltration (48). VEGF induces the migration of VEGF-receptor 1–positive (VEGFR1–positive) and Flt-1–positive myelomonocytic cells (2, 49). Cursiefen et al. reported that VEGF functions in macrophage infiltration in injury-induced neovasculture in mouse corneas (19). Here, the VEGF-induced angiogenesis in mouse corneas was reduced by approximately 50% 6 days after Cl<sub>2</sub>MDP-LIP treatment, and IL-1β–induced angiogenesis was blocked. VEGF-induced angiogenesis in mouse corneas might be partly due to the infiltration of macrophages: 2- to 3-fold increases occurred in monocyte/macrophage infiltration on days 4 and 6 after VEGF treatment, which might function in angiogenesis. VEGF- but not MCP-1-induced chemotaxis of human monocytes was inhibited by the VEGF receptor tyrosine kinase inhibitor SU5416 through Flt-1 (50). We recently confirmed that SU5416 partially blocked IL-1β–induced angiogenesis in mouse corneas (31).

COX-2 is pivotal in IL-1β–induced angiogenesis in vitro and in vivo (31). The enhanced production of prostanoids, such as PGE<sub>2</sub> and thromboxane A<sub>2</sub> (TXA<sub>2</sub>), in response to IL-1β could promote angiogenesis, suggesting a model in which IL-1β–induced angiogenesis is mediated through both prostanoids and angiogenic factors (31). Pold et al. reported that COX-2 upregulated the expression of CXCL8 (IL-8) and CXCL5 (ENA-78) in non-small cell lung cancer cells in vitro and in vivo (38). The IL-1β–induced upregulation of IL-8 in lung cancer cells was blocked by anti-PGE<sub>2</sub> mAb (38). KC and VEGF-A were decreased in IL-1β–implanted corneas treated with DFU (Figure 9, G and H). This inflammatory cytokine-induced angiogenesis might be partially attributable to upregulation of VEGF-A and KC through the COX-2–activation pathway. CXC chemokines are known to induce angiogenesis (35). Addison et al. demonstrated the angiogenic activity of ELR<sup>+</sup> CXC chemokines through CXCR2 (36). Saijo et al. showed that treatment with anti-CXCR2 Ab inhibited IL-1β–induced tumor growth in mice (6). Keane et al. demonstrated that CXC chemokines modulated tumor growth through angiogenesis by indirect effects on tumor cells or leukocytes in CXCR2<sup>-/-</sup> mice (51). Our corneal model revealed that IL-1β increased the expression of both CXC chemokines and VEGF-A (Figure 9). Furthermore, IL-1β–induced



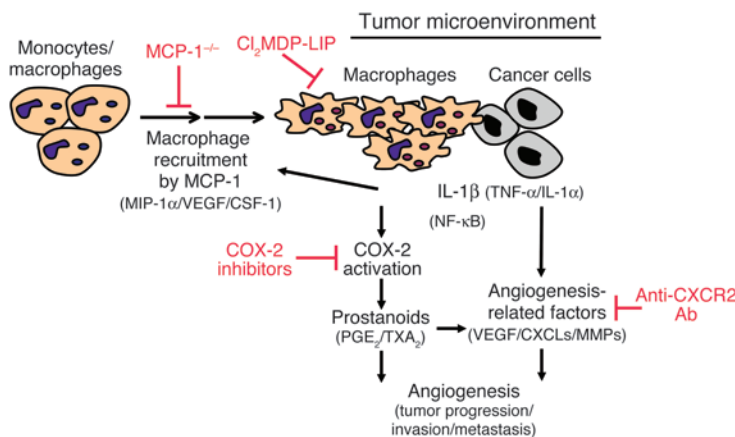


**Figure 10**

Model of the involvement of macrophages in IL-1 $\beta$ -induced angiogenesis in the tumor microenvironment. Monocytes/macrophages are expected to be recruited to the tumor environment in response to IL-1 $\beta$  and possibly other chemokines that attract macrophages. COX-2 activation is then induced, and the macrophages promote angiogenesis and tumor progression. Signaling molecules downstream of COX-2, PGE<sub>2</sub>, and TXA<sub>2</sub> enhance the production of various angiogenesis-related factors (37, 38). IL-1 $\beta$ , IL-1 $\alpha$ , and TNF- $\alpha$  enhance the expression of angiogenesis-related factors in cancer and vascular endothelial cells resulting from autocrine and/or paracrine controls in angiogenesis (5, 30, 55, 56). Monocytes/macrophages are recruited to the tumor environment in response to MCP-1 (and possibly MIP-1 $\alpha$ , VEGF/PIGF, and CSF-1) accompanied by COX-2 activation in infiltrating macrophages by IL-1 $\beta$  (and possibly IL-1 $\alpha$  and/or TNF- $\alpha$ ). As a result, angiogenesis is enhanced by prostanoids (such as PGE<sub>2</sub> and TXA<sub>2</sub>) as well as other angiogenic factors (such as VEGF, CXC chemokines, and MMPs). Clodronate blocks inflammatory angiogenesis induced by IL-1 $\beta$ .

corneal angiogenesis was partially inhibited by anti-CXCR2 Ab. CXC chemokines, prostanoids, and VEGF-A could therefore all be involved in IL-1 $\beta$ -induced angiogenesis.

Many COX-2-positive cells infiltrate the IL-1 $\beta$ -induced neovasculature in mouse corneas (31). Here, macrophage infiltration was enhanced in response to IL-1 $\beta$  compared with VEGF. Infiltrating macrophages around the IL-1 $\beta$ -induced neovasculature expressed COX-2, whereas those surrounding preexisting vessels did not. The number of infiltrating macrophages was higher in LLC/IL-1 $\beta$  tumors than in LLC/neo tumors in vivo. Our study revealed several features of the role of COX-2 production in tumor angiogenesis. LLC/IL-1 $\beta$ -induced angiogenesis in vivo was blocked by a COX-2 inhibitor. LLC/IL-1 $\beta$  tumor growth and induced microvascularization were specifically blocked by the COX-2 inhibitor. Macrophage infiltration in LLC/IL-1 $\beta$ -induced tumors was significantly blocked by a COX-2 inhibitor compared with wild-type mice. These findings suggest that IL-1 $\beta$ -driven tumor angiogenesis and tumor growth depend on macrophage infiltration as well as COX-2-positive tumor-associated macrophages and possibly cancer cells with high COX-2 expression (Figure 10). However, inhibition of COX-2 activity only weakly influenced macrophage infiltration in response to IL-1 $\beta$  in cancer (Figure 8). The decrease in angiogenesis and tumor growth by LLC/IL-1 $\beta$  induced by a COX-2 inhibitor could be specifically associated with COX-2 activity in macrophages and other cell types rather than the number of infiltrating macrophages at or near the site of tumor growth. The infiltration of tumor-associated or tumor-educated macrophages is often associated with disease progression or poor prognosis for

cancer patients. These activated macrophages appear to be important in tumor angiogenesis (16, 30, 46, 52). An experimental model system with LLC/IL-1 $\beta$  showed IL-1 $\beta$  to be essential for tumor angiogenesis, invasion, and metastasis as well as immunosuppression (6–8). COX-2-positive macrophages activated in the inflammatory microenvironment might be critical for acquiring a malignant phenotype in cancer. COX-2-positive macrophages could thus be target cells for future anticancer therapeutic strategies.

In conclusion, IL-1 $\beta$  induced angiogenesis with a concomitant infiltration of macrophages, most of which were COX-2 positive. Macrophage depletion through treatment with a targeted drug or using MCP-1 $^{-/-}$  mice abrogated IL-1 $\beta$ -induced angiogenesis. This complex process involves multiple redundant and interconnected pathways. It is therefore remarkable that macrophage depletion alone almost abolished IL-1 $\beta$ -induced corneal neovascularization and tumor growth.

## Methods

**Animals.** All animal experiments were approved by the Committee on the Ethics of Animal Experiments, Kyushu University Graduate School of Medical Sciences, Japan. Male BALB/c and C57BL/6 mice (6–10 weeks old) were purchased from Seac Yoshitomi Ltd. MCP-1 $^{-/-}$  mice were kindly provided by B.J. Rollins (Harvard Medical School, Boston, Massachusetts, USA).

**Corneal micropocket assay in mice.** The mouse corneal micropocket assay and quantification of neovascularization were performed as described previously (31, 53).

**Immunohistochemistry.** Mice were sacrificed under deep anesthesia with pentobarbital sodium (60 mg/kg i.p.). The eyes were removed, snap-frozen in OCT compound (Sakura Finetech Co.), and 5- $\mu$ m sections were cut, air dried, and fixed in cold acetone for 10 minutes. The sections were blocked with 3% BSA and labeled at room temperature with rat anti-mouse Gr-1 (550291) or rat anti-mouse CD31 (550274; BD Biosciences) for 1 hour, followed by biotinylated goat anti-rat Ig (559286; BD Biosciences) for 20 minutes. Frozen sections were labeled with biotinylated anti-F4/80 for 1 hour. The sections were treated with horseradish peroxidase-conjugated streptavidin (1:1000; Jackson ImmunoResearch Laboratories Inc.) and 3,3'-diaminobenzidine substrate (BioGenex Laboratories). Frozen sections were also stained with rat anti-mouse F4/80 (MCA497R; Serotec) or anti-Gr-1 and rabbit anti-mouse COX-2 Ab (160126; Cayman Chemical Co.).

**Isolation of cornea-infiltrating cells and flow cytometry.** Inflammatory cells were isolated from the corneas as described previously (54). For 3-color flow cytometry, corneal infiltrating cells were stained with the following: PE-CD11b mAb (RM2804; CALTAG Laboratories) to label macrophages and neutrophils or PE-anti-CD11c mAb (557401; BD Biosciences) to label dendritic cells; either FITC-anti-Gr-1 (551460; BD Biosciences) to label neutrophils or FITC-anti-F4/80 mAb (RM2901; CALTAG Laboratories) to label macrophages; and propidium iodide (BD Biosciences).

**ELISAs.** Groups of 4 corneas were removed and dissected with scissors. The supernatants were assayed in ELISA kits for mouse MCP-1 (KMC1010-SB; BioSource International), mouse KC (MKC00B; R&D Systems), mouse MIP-2 (MM200; R&D Systems), and mouse VEGF-A (MMV00; R&D Systems).

**Liposomes.** Cl<sub>2</sub>MDP-LIPs were prepared as previously described (23). Animals received 200  $\mu$ l Cl<sub>2</sub>MDP-LIPs or PBS-LIPs i.v. in the retro-orbital plexus with a 26-gauge needle on days -2, 0, 2, and 4. They also received 10



μl Cl<sub>2</sub>MDP-LIPs in 1 eye and 10 μl PBS-LIPs in the other, injected into the s.c. space. All injections were masked.

**Mouse dorsal air sac assay.** A dorsal air sac assay was performed according to the method published previously (50). Five mice in each group were sacrificed and skinned on day 6. We counted the number of meandering blood vessels within the chamber in the area of the air sac fascia and graded the angiogenic response from 0 to 5, respectively.

**Quantitative real-time RT-PCR.** Total RNA was extracted from 6 corneas by ISOGEN (317-02503; Nippon Gene Co.), and quantitative RT-PCR was performed in duplicate using mouse ENA-78-specific TaqMan primers and probes and the ABI Prism 7300 sequence detector (Applied Biosystems).

**Statistics.** All results are expressed as mean ± SEM. The statistical significance of differences between groups was analyzed by 2-tailed Student's *t* test or Mann-Whitney *U* test. Differences were considered significant at *P* < 0.05, and each experiment was performed at least twice.

1. Carmeliet, P. 2003. Angiogenesis in health and disease. *Nat. Med.* **9**:653–660.
2. Rafii, S., and Lyden, D. 2003. Therapeutic stem and progenitor cell transplantation for organ vascularization and regeneration. *Nat. Med.* **9**:702–712.
3. Dinarello, C.A. 1996. Biologic basis for interleukin-1 in disease. *Blood.* **87**:2095–2147.
4. Mantovani, A., Bussolino, F., and Dejana, E. 1992. Cytokine regulation of endothelial cell function. *FASEB J.* **6**:2591–2599.
5. Torisu, H., et al. 2000. Macrophage infiltration correlates with tumor stage and angiogenesis in human malignant melanoma: possible involvement of TNFalpha and IL-1alpha. *Int. J. Cancer.* **85**:182–188.
6. Saijo, Y., et al. 2002. Proinflammatory cytokine IL-1 beta promotes tumor growth of Lewis lung carcinoma by induction of angiogenic factors: in vivo analysis of tumor-stromal interaction. *J. Immunol.* **169**:469–475.
7. Yano, S., et al. 2003. Multifunctional interleukin-1beta promotes metastasis of human lung cancer cells in SCID mice via enhanced expression of adhesion-, invasion- and angiogenesis-related molecules. *Cancer Sci.* **94**:244–252.
8. Voronov, E., et al. 2003. IL-1 is required for tumor invasiveness and angiogenesis. *Proc. Natl. Acad. Sci. U. S. A.* **100**:2645–2650.
9. Bar, D., Apte, R.N., Voronov, E., Dinarello, C.A., and Cohen, S.A. 2004. Continuous delivery system of IL-1 receptor antagonist reduces angiogenesis and inhibits tumor development. *FASEB J.* **18**:161–163.
10. Song, X., et al. 2003. Differential effects of IL-1 alpha and IL-1 beta on tumorigenicity patterns and invasiveness. *J. Immunol.* **171**:6448–6456.
11. Shaw, J.P., Chuang, N., Yee, H., and Shamamian, P. 2003. Polymorphonuclear neutrophils promote rFGF-2-induced angiogenesis in vivo. *J. Surg. Res.* **109**:37–42.
12. Fuentes, M.E., et al. 1995. Controlled recruitment of monocytes and macrophages to specific organs through transgenic expression of monocyte chemoattractant protein-1. *J. Immunol.* **155**:5769–5776.
13. Lu, B., et al. 1998. Abnormalities in monocyte recruitment and cytokine expression in monocyte chemoattractant protein 1-deficient mice. *J. Exp. Med.* **187**:601–608.
14. Huang, D.R., Wang, J., Kivisakk, P., Rollins, B.J., and Ransohoff, R.M. 2001. Absence of monocyte chemoattractant protein 1 in mice leads to decreased local macrophage recruitment and antigen-specific T helper cell type 1 immune response in experimental autoimmune encephalomyelitis. *J. Exp. Med.* **193**:713–726.
15. Low, Q.E., et al. 2001. Wound healing in MIP-1 alpha(-/-) and MCP-1(-/-) mice. *Am. J. Pathol.*

**Acknowledgments**

We thank R. Kono, T. Oshima, M. Imamura, and M. Takahara (Kyushu University) for technical support and N. Shinbaru (Kyushu University) for editorial help. This work was supported by the Third-Term Comprehensive Ten-Year Strategy for Cancer Control from the Ministry of Health, Welfare, and Labor of Japan.

Received for publication September 4, 2004, and accepted in revised form August 23, 2005.

Address correspondence to: Mayumi Ono, Department of Medical Biochemistry, Graduate School of Medical Science, Kyushu University, 3-1-1 Maidashi, Higashi-ku, Fukuoka 812-8582, Japan. Phone: 81-92-642-6098; Fax: 81-92-642-6203; E-mail: mayumi@biochem1.med.kyushu-u.ac.jp.

- 159:457–463.
16. Coussens, L.M., and Werb, Z. 2002. Inflammation and cancer. *Nature.* **420**:860–867.
17. Tsutsumi, C., et al. 2003. The critical role of ocular-infiltrating macrophages in the development of choroidal neovascularization. *J. Leukoc. Biol.* **74**:25–32.
18. Moulton, K.S., et al. 2003. Inhibition of plaque neovascularization reduces macrophage accumulation and progression of advanced atherosclerosis. *Proc. Natl. Acad. Sci. U. S. A.* **100**:4736–4741.
19. Cursiefen, C., et al. 2004. VEGF-A stimulates lymphangiogenesis and hemangiogenesis in inflammatory neovascularization via macrophage recruitment. *J. Clin. Invest.* **113**:1040–1050. doi:10.1172/JCI200420465.
20. Leek, R.D., et al. 1996. Association of macrophage infiltration with angiogenesis and prognosis in invasive breast carcinoma. *Cancer Res.* **56**:4625–4629.
21. Toi, M., et al. 1999. Significance of thymidine phosphorylase as a marker of protumor monocytes in breast cancer. *Clin. Cancer Res.* **5**:1131–1137.
22. Nishie, A., et al. 1999. Macrophage infiltration and heme oxygenase-1 expression correlate with angiogenesis in human gliomas. *Clin. Cancer Res.* **5**:1107–1113.
23. Lissbrant, I.F., et al. 2000. Tumor associated macrophages in human prostate cancer: relation to clinicopathological variables and survival. *Int. J. Oncol.* **17**:445–451.
24. Salvesen, H.B., and Akslen, L.A. 1999. Significance of tumour-associated macrophages, vascular endothelial growth factor and thrombospondin-1 expression for tumour angiogenesis and prognosis in endometrial carcinomas. *Int. J. Cancer.* **84**:538–543.
25. Fujimoto, J., Sakaguchi, H., Aoki, I., and Tamaya, T. 2000. Clinical implications of expression of interleukin 8 related to angiogenesis in uterine cervical cancers. *Cancer Res.* **60**:2632–2635.
26. Koukourakis, M.I., et al. 1998. Different patterns of stromal and cancer cell thymidine phosphorylase reactivity in non-small-cell lung cancer: impact on tumour neoangiogenesis and survival. *Br. J. Cancer.* **77**:1696–1703.
27. Hanada, T., et al. 2000. Prognostic value of tumor-associated macrophage count in human bladder cancer. *Int. J. Urol.* **7**:263–269.
28. Torisu-Itakura, H., Furue, M., Kuwano, M., and Ono, M. 2000. Co-expression of thymidine phosphorylase and heme oxygenase-1 in macrophages in human malignant vertical growth melanomas. *Jpn. J. Cancer Res.* **91**:906–910.
29. Sunderkotter, C., Steinbrink, K., Goebeler, M., Bhardwaj, R., and Sorg, C. 1994. Macrophages and angiogenesis. *J. Leukoc. Biol.* **55**:410–422.
30. Ono, M., Torisu, H., Fukushi, J., Nishie, A., and Kuwano, M. 1999. Biological implications of macrophage infiltration in human tumor angiogenesis. *Cancer Chemother. Pharmacol.* **43**(Suppl.):S69–S71.
31. Kuwano, T., et al. 2004. Cyclooxygenase 2 is a key enzyme for inflammatory cytokine induced angiogenesis. *FASEB J.* **18**:300–310.
32. Sica, A., et al. 1990. Monocyte chemotactic and activating factor gene expression induced in endothelial cells by IL-1 and tumor necrosis factor. *J. Immunol.* **144**:3034–3038.
33. Van Rooijen, N., and Sanders, A. 1994. Liposome mediated depletion of macrophages: mechanism of action, preparation of liposomes and applications. *J. Immunol. Methods.* **174**:83–93.
34. Sakurai, E., Anand, A., Ambati, B.K., van Rooijen, N., and Ambati, J. 2003. Macrophage depletion inhibits experimental choroidal neovascularization. *Invest. Ophthalmol. Vis. Sci.* **44**:3578–3585.
35. Strieter, R.M., et al. 1995. The functional role of the 'ELR' motif in CXC chemokine-mediated angiogenesis. *J. Biol. Chem.* **270**:27348–27357.
36. Addison, C.L., et al. 2000. The CXC chemokine receptor 2, CXCR2, is the putative receptor for ELR+ CXC chemokine-induced angiogenic activity. *J. Immunol.* **165**:5269–5277.
37. Williams, C.S., Tsujii, M., Reese, J., Dey, S.K., and DuBois, R.N. 2000. Host cyclooxygenase-2 modulates carcinoma growth. *J. Clin. Invest.* **105**:1589–1594.
38. Pold, M., et al. 2004. Cyclooxygenase-2-dependent expression of angiogenic CXC chemokines ENA-78/CXC ligand (CXCL) 5 and interleukin-8/CXCL8 in human non-small cell lung cancer. *Cancer Res.* **64**:1853–1860.
39. Li, B.Y., et al. 1992. Human ovarian epithelial cancer cell cultures in vitro express both interleukin 1 alpha and beta genes. *Cancer Res.* **52**:2248–2252.
40. Yoshida, N., et al. 2002. Interleukin-6, tumour necrosis factor alpha and interleukin-1beta in patients with renal cell carcinoma. *Br. J. Cancer.* **86**:1396–1400.
41. Kabir, S., and Daar, G.A. 1995. Serum levels of interleukin-1, interleukin-6 and tumour necrosis factor-alpha in patients with gastric carcinoma. *Cancer Lett.* **95**:207–212.
42. Conejo-Garcia, J.R., et al. 2004. Tumor-infiltrating dendritic cell precursors recruited by a beta-defensin contribute to vasculogenesis under the influence of Vegf-A. *Nat. Med.* **10**:950–958.
43. Zhang, Y., et al. 2002. APCs in the liver and spleen recruit activated allogeneic CD8+ T cells to elicit hepatic graft-versus-host disease. *J. Immunol.* **169**:7111–7118.
44. Cheng, H., et al. 2000. Role of macrophages in restricting herpes simplex virus type 1 growth after ocular infection. *Invest. Ophthalmol. Vis. Sci.* **41**:1402–1409.
45. Ogawa, S., et al. 1999. Induction of macrophage inflammatory protein-1alpha and vascular endothelial growth factor during inflammatory





- neovascularization in the mouse cornea. *Angiogenesis*. **3**:327–334.
46. Ueno, T., et al. 2000. Significance of macrophage chemoattractant protein-1 in macrophage recruitment, angiogenesis, and survival in human breast cancer. *Clin. Cancer Res.* **6**:3282–3289.
47. Fantuzzi, L., et al. 1999. Loss of CCR2 expression and functional response to monocyte chemoattractant protein (MCP-1) during the differentiation of human monocytes: role of secreted MCP-1 in the regulation of the chemotactic response. *Blood*. **94**:875–883.
48. Lyden, D., et al. 2001. Impaired recruitment of bone-marrow-derived endothelial and hematopoietic precursor cells blocks tumor angiogenesis and growth. *Nat. Med.* **7**:1194–1201.
49. Sawano, A., et al. 2001. Flt-1, vascular endothelial growth factor receptor 1, is a novel cell surface marker for the lineage of monocyte-macrophages in humans. *Blood*. **97**:785–791.
50. Itokawa, T., et al. 2002. Antiangiogenic effect by SU5416 is partly attributable to inhibition of Flt-1 receptor signaling. *Mol. Cancer Ther.* **1**:295–302.
51. Keane, M.P., Belperio, J.A., Xue, Y.Y., Burdick, M.D., and Strieter, R.M. 2004. Depletion of CXCR2 inhibits tumor growth and angiogenesis in a murine model of lung cancer. *J. Immunol.* **172**:2853–2860.
52. Pollard, J.W. 2004. Tumour-educated macrophages promote tumour progression and metastasis. *Nat. Rev. Cancer*. **4**:71–78.
53. Nakao, S., Kuwano, T., Ishibashi, T., Kuwano, M., and Ono, M. 2003. Synergistic effect of TNF-alpha in soluble VCAM-1-induced angiogenesis through alpha 4 integrins. *J. Immunol.* **170**:5704–5711.
54. Sonoda, K., et al. 1998. Inhibition of corneal inflammation by the topical use of Ras farnesyltransferase inhibitors: selective inhibition of macrophage localization. *Invest. Ophthalmol. Vis. Sci.* **39**:2245–2251.
55. Ryuto, M., et al. 1996. Induction of vascular endothelial growth factor by tumor necrosis factor alpha in human glioma cells. Possible roles of SP-1. *J. Biol. Chem.* **271**:28220–28228.
56. Yoshida, S., et al. 1997. Involvement of interleukin-8, vascular endothelial growth factor, and basic fibroblast growth factor in tumor necrosis factor alpha-dependent angiogenesis. *Mol. Cell. Biol.* **17**:4015–4023.